Tree Physiology Advance Access published April 14, 2015

Tree Physiology 00, 1–15
doi:10.1093/treephys/tpv027

Research paper

Overexpression of a *Populus trichocarpa* H$^+$-pyrophosphatase gene *PtVP1.1* confers salt tolerance on transgenic poplar

Y. Yang[1,2], R.J. Tang[2,5], B. Li[2], H.H. Wang[2], Y.L. Jin[2], C.M. Jiang[2], Y. Bao[2], H.Y. Su[1], N. Zhao[3], X.J. Ma[3], L. Yang[4], S.L. Chen[3], X.H. Cheng[1,6] and H.X. Zhang[1,2,6]

[1]College of Agriculture, Ludong University, 186 Hongqizhong Road, Yantai, China 264025; [2]National Key Laboratory of Plant Molecular Genetics, Shanghai Institute of Plant Physiology and Ecology, Chinese Academy of Sciences, 300 Fenglin Road, Shanghai, China 200032; [3]College of Biological Sciences and Technology, Beijing Forestry University, 35 Qinghua-East Road, Beijing, China 100083; [4]College of Life Sciences, Nanjing University, 22 Hankou Road, Nanjing, China 210093; [5]Present address: Department of Plant and Microbial Biology, University of California, Berkeley, CA 94720, USA; [6]Corresponding authors (chengxianhao@sohu.com; hxzhang@sippe.ac.cn)

Received January 7, 2015; accepted March 8, 2015; handling Editor Chunyang Li

The *Arabidopsis* vacuolar H$^+$-pyrophosphatase (*AVP1*) has been well studied and subsequently employed to improve salt and/or drought resistance in herbaceous plants. However, the exact function of H$^+$-pyrophosphatase in woody plants still remains unknown. In this work, we cloned a homolog of type I H$^+$-pyrophosphatase gene, designated as *PtVP1.1*, from *Populus trichocarpa*, and investigated its function in both *Arabidopsis* and poplar. The deduced translation product PtVP1.1 shares 89.74% identity with AVP1. Semi-quantitative reverse transcription polymerase chain reaction (RT-PCR) and quantitative real-time PCR analyses revealed a ubiquitous expression pattern of *PtVP1.1* in various tissues, including roots, stems, leaves and shoot tips. Heterologous expression of *PtVP1.1* rescued the retarded-root-growth phenotype of *avp1*, an *Arabidopsis* knock out mutant of *AVP1*, on low carbohydrate medium. Overexpression of *PtVP1.1* in poplar (*P. davidiana* × *P. bolleana*) led to more vigorous growth of transgenic plants in the presence of 150 mM NaCl. Microsomal membrane vesicles derived from *PtVP1.1* transgenic plants exhibited higher H$^+$-pyrophosphatase hydrolytic activity than those from wild type (WT). Further studies indicated that the improved salt tolerance was associated with a decreased Na$^+$ and increased K$^+$ accumulation in the leaves of transgenic plants. Na$^+$ efflux and H$^+$ influx in the roots of transgenic plants were also significantly higher than those in the WT plants. All these results suggest that *PtVP1.1* is a functional counterpart of AVP1 and can be genetically engineered for salt tolerance improvement in trees.

Keyword: *Arabidopsis*, Na$^+$ and K$^+$ distribution, transgenic plants.

Introduction

Salinity is one of the major abiotic stresses that adversely affect plant growth and productivity in modern agriculture (Wang et al. 2001). Therefore, engineering new plant species with improved salt resistance has been raised as an important agronomic issue worldwide. Higher plants have developed a series of mechanisms to reduce the injuries imposed by excessive sodium ions in the cytoplasm. The compartmentalization of Na$^+$ into vacuoles and the exclusion of Na$^+$ from cells by the plasma membrane-located Na$^+$/H$^+$ antiporters provide an efficient mechanism for averting the toxic effects of Na$^+$ in the cytosol (Shi et al. 2003, Mishra et al. 2015). The Na$^+$ compartmentalization process is mediated by vacuolar Na$^+$/H$^+$ antiporters that are driven by H$^+$ electrochemical gradient across the tonoplast generated by the vacuolar H$^+$ pump, including vacuolar H$^+$-ATPase and H$^+$-pyrophosphatase (Blumwald and Gelli 1997). Plant vacuolar-type inorganic pyrophosphatases (H$^+$-PPase) utilize the energy of inorganic pyrophosphate (PPi) hydrolysis as the driving force for H$^+$ movement across biological membranes, and are highly conserved among different plant species (Drozdowicz and Rea 2001). Prototypical plant H$^+$-PPases are divided into two phylogenetically distinct types, depending on their sensitivity to K$^+$. Plant type I H$^+$-PPases, which were first

isolated from vacuoles, depend on cytosolic K^+ for their maximum activity and are moderately sensitive to the inhibition of Ca^{2+} (Rea and Poole 1985, Rea et al. 1992, Maeshima 2000). It was reported that both PPi hydrolysis and PPi-dependent proton pumping activities of H^+-PPases in rye plants grown under mineral-deficient conditions such as K^+, NO_3^-, Ca^{2+}-deficiency were greater than in those grown under normal conditions (Kasai et al. 1998).

In principle, enhanced expression of vacuolar H^+-PPases should increase the sequestration of ions in the vacuole by increasing the H^+ movement across biological membranes (Gaxiola et al. 2001). In practice, overexpression of *AVP1* coding for a single subunit protein of type I vacuolar H^+-PPase from *Arabidopsis*, and other plant type I H^+-PPase genes, increased both salt and drought tolerance in diverse systems, including *Arabidopsis* (*Arabidopsis thaliana*; Gaxiola et al. 2001), tomato (*Lycopersicon esculentum*; Park et al. 2005), tobacco (*Nicotiana tabacum*; Gao et al. 2006, Duan et al. 2007), rice (*Oryza sativa*; Zhao et al. 2006), cotton (*Gossypium hirsutum*; Lv et al. 2008, 2009), alfalfa (*Medicago sativa*; Bao et al. 2009), maize (*Zea mays*; Li et al. 2008) and creeping bentgrass (*Agrostis stolonifera*; Li et al. 2010). Furthermore, up-regulation of *AVP1* also enhanced root and shoot biomass, photosynthetic capacity and nutrient uptake by affecting the abundance and the activity of PM H^+-ATPase in a manner correlated with apoplastic pH alterations and rhizosphere acidification. These phenotypes have been observed in a variety of agriculturally important crops grown under normal or limited nutrient conditions, such as low Pi and NO_3^- (Li et al. 2005, Yang et al. 2007, Paez-Valencia et al. 2013).

Although all these previous studies have highlighted the important roles of H^+-PPases in herbaceous plants, very little is known about the possible roles of this kind of H^+ pump in trees. *Populus* has been studied as an important model of woody plants because of its worldwide distribution, genotype diversity, economic and ecological relevance, sequenced genome and easier genetic manipulation (Jansson and Douglas 2007). In this work, we cloned a type I H^+-pyrophosphatase homolog *PtVP1.1* from *Populus trichocarpa* and investigated its function in both *Arabidopsis* and poplar. We also generated transgenic poplar (*P. davidiana* × *P. bolleana*) overexpressing *PtVP1.1* to test its potential application in the engineering of salt-tolerant woody plants. Our results indicate that constitutive expression of *PtVP1.1* can significantly enhance the resistance of transgenic poplar plants to salt, and the improved salt tolerance was associated with the augmented PPi hydrolytic activities, the decreased Na^+ and increased K^+ accumulation, and the improved Na^+ efflux and H^+ influx in transgenic plants.

Materials and methods

Plant materials and growth conditions

Arabidopsis thaliana ecotype Col-0 was used in this study. *avp1* (GK-596F06-025557) was obtained from GABI-KAT (http://www.gabi-kat.de/). Homozygous *avp1* mutant was identified using gene-specific and T-DNA left border primers (see Table S1 available as Supplementary Data at *Tree Physiology* Online).

Arabidopsis seeds were sterilized with 10% sodium hypochlorite for 5 min and washed three times with sterilized water, and then plated on MS medium (Murashige and Skoog 1962) supplemented with 2% sucrose (or 0.2% sucrose for low carbohydrate phenotypic assay) and 0.8% agar. Seeds were stratified at 4 °C for 2 days and then transferred to 22 °C for another 7 days before they were transferred to soil and grown in greenhouse at 21–23 °C under 12 h light/12 h dark cycles.

Populus trichocarpa genotype Nisqually-1 and Shanxin yang (*P. davidiana* × *P. bolleana*) used in this study were propagated and cultivated as described previously (Wang et al. 2011). Initially, poplar materials were amplified and kept by aseptically transferring shoot apices to fresh MS medium supplemented with 0.1 mg l^{-1} naphthaleneacetic acid. Plantlets were grown in glass bottles in the culture room with cool white fluorescent light (~200 μmol m^{-2} s^{-1}) under 12 h light/12 h dark photoperiod at 21–25/15–18 °C (day/night). One-month-old plantlets were transferred to soil and kept in greenhouse under 14 h photoperiod comprising natural daylight supplemented with lamps (120–150 μEm^{-2} s^{-1}) at ~21–25/15–18 °C (day/night).

Subcellular localization studies

To determine the subcellular localization of PtVP1.1, the coding region of *PtVP1.1* was in-frame fused to the 3′-terminal of cyan fluorescent protein (CFP) sequence via the SmaI-SpeI site in the pA7-CFP plasmid and transferred into poplar mesophyll protoplasts or *A. thaliana* plant system biology dark-type culture (PSBD) protoplasts by polyethylene glycol-mediated transfection as described previously (Miao and Jiang 2007, Tang et al. 2014). Cyan fluorescent protein fluorescence was imaged after the protoplasts were incubated at 23 °C for 16 h by the confocal laser scanning microscope at 458 nm wavelength (Carl Zeiss LSM 510; META, Dresden, Germany).

Plant transformation

To produce the gain-of-function allele of *PtVP1.1* gene (*PtVP1.1m*), a Glu^{227}-to-Asp mutation was introduced into *PtVP1.1* by PCR-based Site-Directed Mutagenesis Kit (Stratagene, La Jolla, CA, USA) using the designated primers (see Table S1 available as Supplementary Data at *Tree Physiology* Online). Then, pKS-*PtVP1.1m* plasmid was digested with SmaI and SalI to release the *PtVP1.1m* coding sequence, and inserted into a modified pCAMBIA-2301 vector downstream of the cauliflower mosaic virus 35S promoter. The resultant construct was introduced into *Arabidopsis* or Shanxin yang by *Agrobacterium*-mediated transformation as described previously (Clough and Bent 1998, Wang et al. 2011). Putative transgenic plants were screened on MS medium containing 30 μg l^{-1} kanamycin and transferred to soil for propagations. Regenerated transgenic

plants were analyzed by PCR with 35S or *PtVP1.1* specific primers (*P35S*, *PtVP1.1RT-F* and *PtVP1.1RT-R*) (see Table S1 available as Supplementary Data at *Tree Physiology* Online).

RT-PCR and quantitative real-time RT-PCR analyses

For the expression pattern analysis of *PtVP1.1* in poplar, total RNA was extracted with the RNAiso Reagent (TaKaRa, Osaka, Japan) from different organs or tissues of 6-month-old wild-type (WT) Shanxin yang, including root (R), elongating internode (EI), thickening stem (TS), juvenile leaf (JL), mature leaf (ML), petiole (Pe) and apical bud (A). Xylem (X) and phloem (P) tissues were simply separated by stripping off the barks with a sharp blade.

To verify the relative expression level of different transgenic lines, total RNA was isolated from leaves of WT and kanamycin-resistant plantlets with the RNAiso Reagent (TaKaRa). After treatment with DNase I (Promega, Madison, WI, USA), a total amount of 2 μg RNA was subjected to reverse transcription reaction using ReverTra Ace (TOYOBO, Osaka, Japan) at 42 °C for 1 h. The resultant cDNA was then used for PCR amplification with gene-specific primers. *ACTIN2* and poplar elongation factor gene *EF1β* were employed as internal control in *Arabidopsis* and poplar, respectively. Quantitative real-time RT-PCR was performed with the SYBR Green Realtime PCR Master Mix (Vazyme Biotech, Nanjing, China) and monitored in real time with the CFX Connect Real-Time System (Bio-Rad, Hercules, CA, USA). Three technical replicas were performed. The relative expression of *PtVP1.1* was calculated based on the comparative threshold cycle method using *ACTIN2* or *EF1β* as a control and normalized to the WT expression values. All primers used in this research are listed in Table S1 available as Supplementary Data at *Tree Physiology* Online.

Salt stress tests of transgenic poplar

To test the salt tolerance of WT and transgenic poplar at the whole-plant level, 1-month-old micro-propagated WT and transgenic plantlets were transplanted to soil. After 6 weeks of acclimation in the greenhouse, WT and transgenic lines with similar size and growth status were divided into two groups. Each group was watered every 3 days with 1/8 MS salt solution supplemented with or without 150 mM NaCl for 3 weeks. At the 15th day after the initiation of salt treatment, leaves of WT and transgenic plants from control and treated groups were sampled separately for the determination of chlorophyll content and malondialdehyde (MDA) concentration using the methods described by Lichtenthaler (1987) and Zhao et al. (1994). At the end of salt treatment, plant height, shoot and root biomass of each individual plant were measured immediately. The root, stem and leaf materials of each plant were harvested separately and were used for Na^+ and K^+ content determination. For survival rate analyses, salt-treated plants were cut ~10 cm above the root–shoot joint, and soil in each pot was washed three times with fresh water (1 l per plant each time). After 2 weeks, plants with new buds were defined as survivors.

Determination of Na^+ and K^+ contents

Plant materials collected from WT and transgenic plants at the end of salt treatment were dried at 80 °C for 48 h. Dried samples (50 mg) were digested with concentrated HNO_3, and Na^+ and K^+ contents in the digested solution were determined with an atomic absorption spectrophotometer (Z-8000; Hitachi, Tokyo, Japan) as described previously (Wang and Zhao 1995).

PPase activity measurements

Leaf microsomal fractions were prepared as described previously (Tang et al. 2012). Leaves of 6-week-old hydroponically grown plants were ground in cold homogenization buffer containing 350 mM sucrose, 70 mM Tris–HCl (pH 8.0), 3 mM Na_2EDTA, 0.2% (w/v) BSA, 1.5% (w/v) PVP-40, 5 mM DTT, 10% (v/v) glycerol, 1 mM PMSF and 1× protease inhibitor mixture (Roche, Penzberg, Germany). The homogenate was filtered through four layers of cheesecloth and centrifuged at 4000*g* for 20 min at 4 °C. The supernatant was filtered through cheesecloth again and then centrifuged at 100,000*g* (XL-70; Beckman, Brea, CA, USA) for 1 h. The resultant microsomal pellet was resuspended in 350 mM sucrose, 10 mM Tris–Mes (pH 7.0), 2 mM DTT and 1× protease inhibitor mixture. PPase activity of 10 μg microsomal membranes was determined as phosphate (Pi) release after 40 min incubation at 28 °C. The PPase activity was assayed in a reaction solution containing 25 mM Tris–Mes (pH 7.5), 2 mM $MgSO_4$, 100 μM Na_2MoO_4, 0.1% Brij 58 and 200 μM $Na_4P_2O_7$. PPase activity was expressed as the difference measured in the absence and presence of 50 mM KCl. For the measurement of inorganic Pi amount, reactions were terminated by adding 40 mM citric acid. Freshly prepared AAM solution [50% (v/v) acetone, 2.5 mM ammoniummolybdate, 1.25 M H_2SO_4] was then added to the reaction, vortexed and colorimetrically examined at 355 nm (UV752N; INESA, Shanghai, China). For the blank value, 10 μg boiled membranes instead of fresh microsomes were used.

H^+ flux assays

The recording protocols were followed as described previously (Sun et al. 2009*a*, 2009*b*, Li et al. 2012). Briefly, pre-pulled and silanized glass micropipettes (diameter 5 ± 1 μm, XY-DJ-01; ~~Xuyue Beijing Science and Technology Co., Ltd, Beijing, China~~) were back-filled with H^+ electrode solution (40 mM KH_2PO_4 and 15 mM NaCl, pH 7.0) to a length of 1.0 cm from the tip. Then the micropipettes were front-filled with 10 μm columns of selective liquid ion exchange cocktails (LIXs; H: Fluka 95293). An Ag/AgCl wire electrode holder (XYEH01-1; ~~Xuyue Beijing Science and Technology Co., Ltd~~) was inserted in the back of the electrode to make electrical contact with the measuring solution. The reference electrode was an Ag/AgCl half-cell (DRIREF-2; World Precision Instruments, Inc., Sarasota, FL, USA) connected to the experimental solution by a 0.5% agarose bridge containing 3.0 M KCl. Prior to the flux measurements, the

microelectrodes were calibrated by the H^+ standard solution: H^+: pH 5.0, 6.0 and 7.0. pH was adjusted to 6.0 with NaOH and HCl in the measuring solution.

Only electrodes with Nernstian slopes 58 ± 5 mV/decade (H^+) were used in our experiments. On the basis of Fick's law of diffusion, the ion flux rate was calculated as $J = -D(dc/dx)$, where J is the ion flux in the x direction, D is the ion diffusion constant in a particular medium and dc/dx is the ion concentration gradient. Data and image acquisition, preliminary processing, control of the three-dimensional electrode positioner and stepper-motor-controlled fine focus of the microscope stage were performed with ASET software (Science Wares, East Falmouth, MA, USA, and Applicable Electronics, Sandwich, MA, USA).

For steady-state flux recording, root segments were rinsed with distilled water and equilibrated in the measuring solution (0.1 mM KCl, 0.1 mM NaCl, 0.1 mM $CaCl_2$ and 0.1 mM $MgCl_2$) for 30 min. Then they were transferred and immobilized on Petri dishes containing 10 ml of fresh measuring solution. After equilibration to the basic solution, the steady-state fluxes of H^+ at the meristematic zone, elongation zone and maturation zone were measured at an interval of 30–50 μm.

The effects of H^+-ATPase inhibitors on H^+ fluxes were also examined in the roots of WT, LP1 and LP9 plants. After 7 days of NaCl treatment (100 mM), roots with apices of 1.0–2.0 cm were sampled from control and salt-treated plants and then incubated in 500 μM sodium orthovanadate (Na_3VO_4) solution for 30 min. The steady flux of H^+ was examined in the measuring solution without the addition of the inhibitor.

For flux data analysis, the micro-Volt differences were exported as raw data before they were imported and converted into net H^+ fluxes by using the program JCal V3.2.1 (a free MS Excel spreadsheet, http://www.youngerusa.com or http://www.ifluxes.com).

Na^+ flux assays

Wild-type and transgenic plants (lines LP1 and LP9) were subjected to a long-term NaCl exposure. Roots were carefully removed from MS agar medium, and exposed to MS mineral solution supplemented with or without 100 mM NaCl for 7 days. The nutrient and saline solution was renewed every 24 h, then the roots of WT and transgenic plants were used for ion flux measurements.

Ion flux profiles were measured with the Non-invasive Micro-test ~~Technique~~ (NMT; NMT-YG-100, Younger USA LLC, Amherst, MA, USA) with ASET 2.0 (Science Wares) and iFluxes 1.0 Software (Younger USA, LLC), which is able to simultaneously integrate and coordinate differential voltage signal collection, motion control and image capture. The standard protocols for Na^+ microelectrode preparation and calculation were described previously (Sun et al. 2009*a*, 2009*b*, Li et al. 2012, Yang et al. 2015).

For steady-state flux recording, root segments with the apices of 15–20 mm in length, excised from non-stressed controls and stressed plants, were rinsed with distilled water and equilibrated in the measuring solution (0.1 mM KCl, 0.1 mM NaCl, 0.1 mM $CaCl_2$ and 0.1 mM $MgCl_2$) for 30 min. Then non-transgenic and transgenic plants roots were transferred and immobilized on Petri dishes containing 10 ml of fresh measuring solution. The measured positions of roots were visualized and defined under the NMT microscope because young roots of sample plants were semitransparent under light (Sun et al. 2009*a*, 2009*b*, Li et al. 2012). After equilibration to the basic solution, the steady-state fluxes of Na^+ at the meristematic zone (~300 μm from the root apex), elongation zone (~400–700 μm from the root apex) and maturation zone (~1000 μm from the root apex) were measured at an interval of 30–50 μm.

In accordance with a previous finding (Chen et al. 2005), we noticed that K^+ and Ca^{2+} in the measuring solution reduced the selectivity of Na^+ microelectrodes filled with commercially available Na^+ liquid ion exchanger (Li et al. 2012). In this study, to reduce the interfering effects of K^+ and Ca^{2+} on Na^+ flux (Cuin et al. 2011), Ca^{2+} and K^+ concentrations in the measuring solution were set to a lower concentration of 0.1 mM (Li et al. 2012).

The inhibitory effect of amiloride (a Na^+/H^+ antiporter-specific inhibitor) on Na^+ flux was examined in WT and transgenic plant roots. The non-stressed and salinized roots were treated with amiloride (50 μM) for 30 min. Then steady-state Na^+ flux was recorded in the measuring solution in the absence of the inhibitor.

The micro-Volt differences were exported as raw data before they were imported and converted into net Na^+ fluxes by using the program JCal V3.2.1 (a free MS Excel spreadsheet, http://www.youngerusa.com or http://www.ifluxes.com).

Statistical analyses and GenBank accession numbers

For statistical analyses, Student's *t*-test was used to generate every *P* value. A *P*-value of <0.05 was considered a statistically significant difference. The tests were one-tailed. The data were normalized and all samples were normally distributed with homogeneity of variance.

The gene abbreviation and GenBank accession numbers are as follows: *AVP1* (*A. thaliana*, NM_101437), *TsVP1* (*Thellungiella salsuginea*, AY436553), *BnVP1* (*Brassica napus*, KC443038), *PtVP1.1* (*P. trichocarpa*, XM_002331026), *PtVP1.2* (*P. trichocarpa*, XM_002325151), *PtVP1.3* (*P. trichocarpa*, XM_002318920), *PtVP1.4* (*P. trichocarpa*, XM_002330213), *Ntppa1* (*N. tabacum*, X83729), *Ntppa2* (*N. tabacum*, X83730), *GhVP1* (*G. hirsutum*, HM370494), *NrAVP1* (*Nicotiana rustica*, DQ630713), *Zmvpp1* (*Z. mays*, NM_001111910), *OVP1* (*O. sativa*, D45383), *OVP2* (*O. sativa*, D45384), *AVP2* (*A. thaliana*, AF182813), *PtSOS1* (*P. trichocarpa*, XM_002315801), *PtNHX1* (*P. trichocarpa*, XM_002307158), *PtNHX2* (*P. trichocarpa*, XM_002319556), *PtNHX4* (*P. trichocarpa*, XM_002315496), *PtCAT2* (*P. trichocarpa*, XM_006382924) and *PtP5CS1* (*P. trichocarpa*, XM_002315166).

Results

Isolation and sequence analysis of PtVP1.1

To dissect the possible role of H$^+$-pyrophosphatase in abiotic stress response of woody plants, we performed homology-based BLAST searches to collect candidate gene sequences coding vacuole type I H$^+$-pyrophosphatases from the Joint Genome Initiative poplar database (JGI, *P. trichocarpa* genome portal v1.1; http://genome.jgi-psf.org/Poptr1_1/Poptr1_1.home.html). Four candidate *AVP1* homologs were identified from the *Populus* genome, designated as *PtVP1.1*, *PtVP1.2*, *PtVP1.3* and *PtVP1.4*. A sequence (2307 bp) encoding *PtVP1.1* was isolated (GenBank accession No. XM_002331026). *PtVP1.1* encodes a 768 amino acid protein (PtVP1.1) with a calculated molecular mass of 80 kDa, which shares the highest identity in amino acid sequence with H$^+$-pyrophosphatases from other higher plants, such as AVP1 (89.74% identity) (Figure 1a). PtVP1, like the other H$^+$-pyrophosphatases from *Arabidopsis*, rice and cotton, contains all the highly conserved domains reported by Drozdowicz and Rea (2001) (Figure 1a). Phylogenetic analysis showed that PtVP1.1 is clustered to type I (K$^+$-sensitive) vacuolar H$^+$-PPases (Figure 1b). Protein structure analysis using TMHMM Server v. 2.0 (http://www.cbs.dtu.dk/services/TMHMM) predicted 13 transmembrane domains (Figure 1c), similar to the other higher plant H$^+$-PPases (Maeshima 2000). This observation is consistent with the putative role of PtVP1.1 that acts as a putative vacuolar H$^+$-PPases in *Populus*.

PtVP1.1 is ubiquitously expressed in Populus

As a first step to understand the possible biological functions of *PtVP1.1*, we performed RT-PCR analysis to determine their relative transcript abundance in various tissues and organs of greenhouse grown Shanxin yang. The results showed that transcript levels of *PtVP1.1* were detectable in all tested materials (Figure 2a). Further quantitative real-time RT-PCR analyses indicated that *PtVP1.1* was ubiquitously expressed in R, EI, TS, X, P, JL, ML, Pe and A, with the highest expression level in xylem tissues (Figure 2b).

Populus PtVP1.1 protein is a functional homolog of AVP1

To further determine the possible function of *PtVP1.1*, an *Arabidopsis* T-DNA insertion line *avp1* (GK-596F06-025557) was characterized. The *avp1* mutant contained a T-DNA insertion in the second exon of *AVP1* (see Figure S1a available as Supplementary Data at *Tree Physiology* Online). A homozygous T_3 *avp1* individual was isolated (see Figure S1b available as Supplementary Data at *Tree Physiology* Online). This insertion abolished the expression of *AVP1* in *avp1*. As confirmed by RT-PCR analyses using *AVP1*-specific primers, *avp1* mutant lacked a detectable level of transcripts for *AVP1* (see Figure S1c and

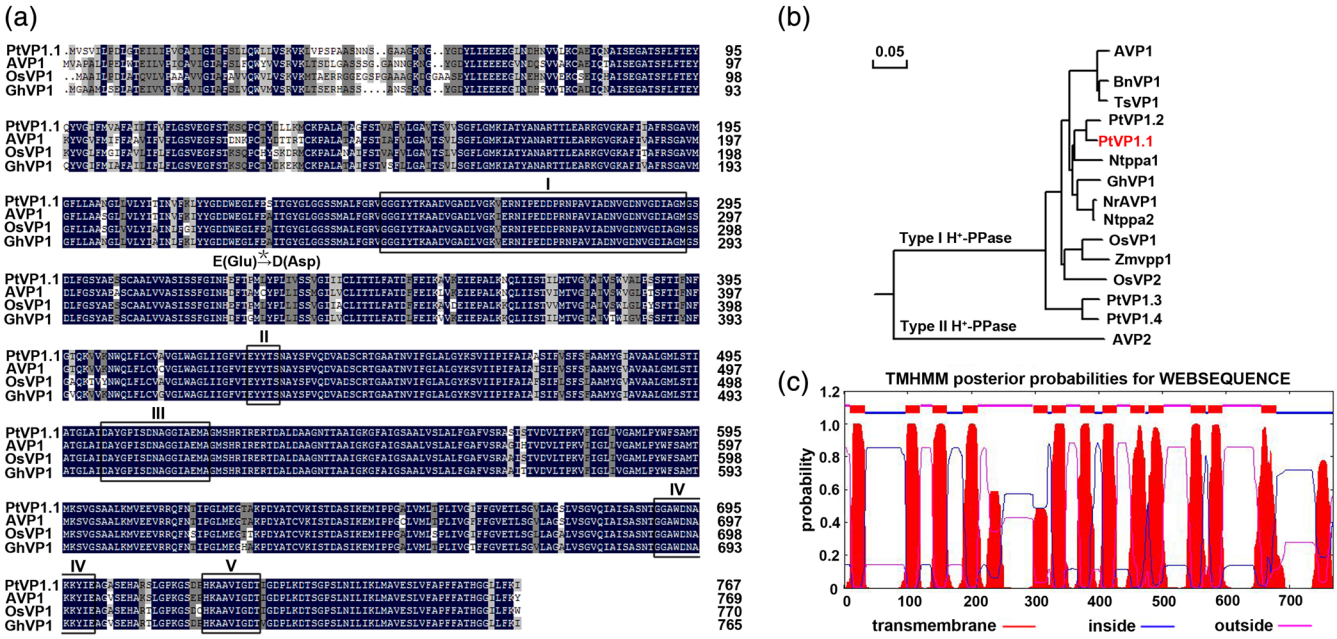

Figure 1. Amino acid sequence alignment and phylogenetic tree of different H$^+$-PPase protein family members. (a) Multiple alignment of the deduced amino acid sequences of H$^+$-PPase proteins from *Populus trichocarpa* (PtVP1.1, XM_002331026), *Arabidopsis thaliana* (AVP1, NM_101437), *Oryza sativa* (OsVP1, D45383) and *Gossypium hirsutum* (GhVP1, No. HM370494). Residues are highlighted in black, dark gray and light gray according to the level of conservation. The highly conserved motifs reported by Drozdowicz and Rea (2001) for H$^+$-PPase proteins are boxed. The Glu^{227}-to-Asp mutation of PtVP1.1 is indicated with an asterisk. (b) Phylogenetic tree of typical vacuolar H$^+$-PPase proteins from various organisms. Phylogram in which the branch lengths are proportional to sequence divergence was conducted with DNAMAN software. (c) The predicted transmembrane domains of PtVP1.1 protein using TMHMM Server v. 2.0 (http://www.cbs.dtu.dk/services/TMHMM).

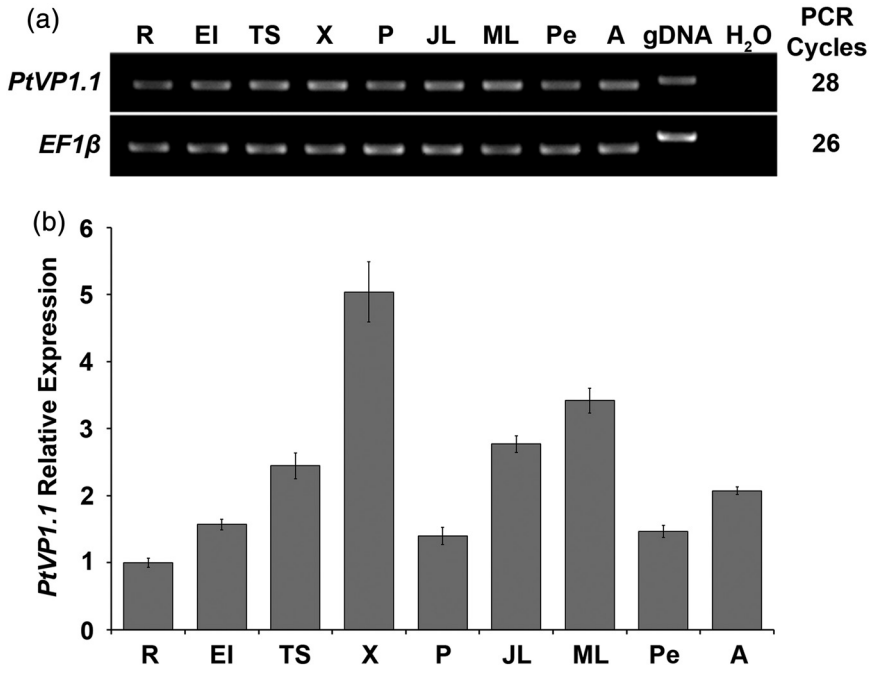

Figure 2. *PtVP1.1* expression pattern in different tissues of Shanxin yang (*Populus davidiana* × *P. bolleana*). (a) RT-PCR analyses. (b) Quantitative real-time PCR analyses. Elongation factor gene *EF1β* was used as an internal control. R, root; EI, elongating internode; TS, thickening stem; X, xylem; P, phloem; JL, juvenile leaf; ML, mature leaf; Pe, petiole; A, apical bud.

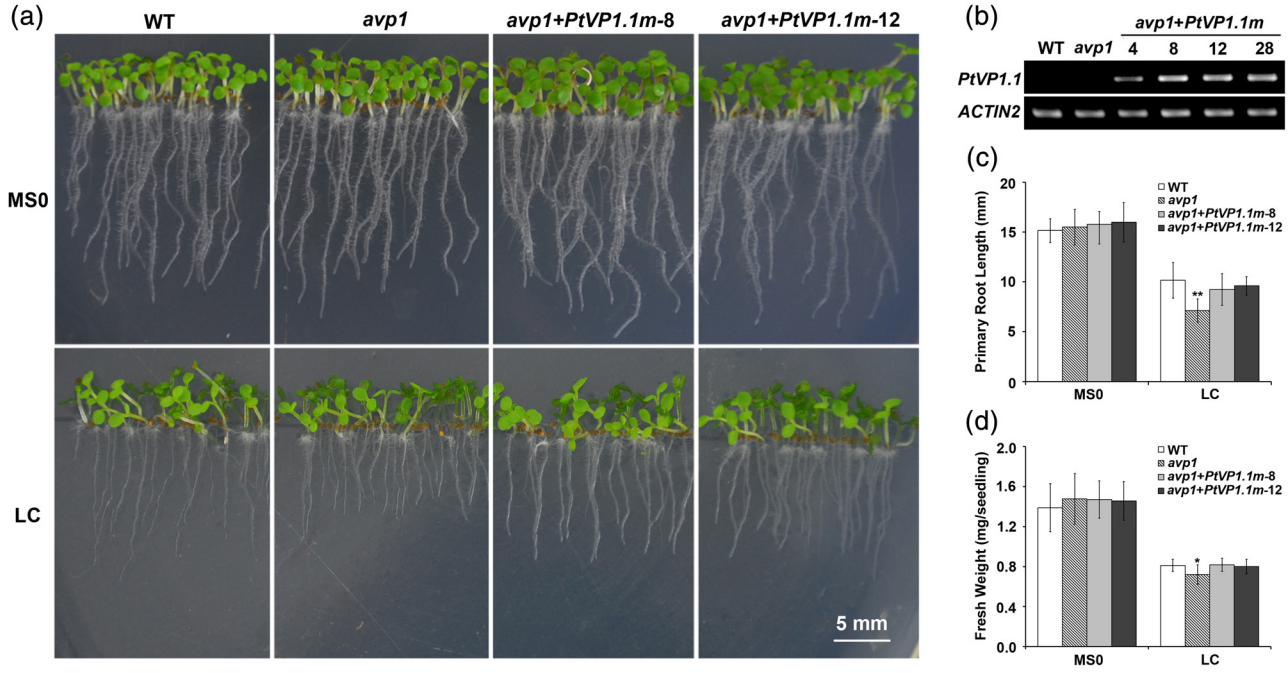

Figure 3. Functional complementation of *Arabidopsis avp1* mutant by *PtVP1.1m*. (a) Growth phenotype of WT, *avp1* and two *PtVP1.1m* complementary lines 8 and 12 on MS medium supplemented with 2% (MS0) or 0.2% (LC) sucrose. Photographs were taken on the fifth day after seeds germinated. (b) RT-PCR analyses of transgene expression in wild type (WT), *avp1* and different *PtVP1.1m* complementary lines. *ACTIN2* gene was used as an internal control. (c and d) Primary root length and shoot fresh weight of seedlings at the end of treatment. Values are means ± SD of 20 individual plants with three independent biological replicates. Scale bars = 5 mm.

Table S1 available as Supplementary Data at *Tree Physiology* Online). Compared with WT plants (Col-0), *avp1* mutant exhibited no obvious phenotypic change during the life cycle when grown under normal nutrient condition (Figures 3a and S1d available as Supplementary Data at *Tree Physiology* Online). However, the growth of *avp1* mutant plants were stunted with

shortened root length and decreased fresh weight when grown under low carbohydrate (0.2% sucrose) conditions (Figure 3c and d).

Previously, an intragenic E229D gain-of-function allele of AVP1 was shown to have an in vitro-coordinated increase of both PPi hydrolytic activity and PPi-dependent H^+ translocation (Zhen et al. 1997). Therefore, we constructed an E227D gain-of-function allele of *PtVP1.1m* gene with a Glu^{227}-to-Asp mutation in PtVP1.1 (Figure 4a). Transformation of *avp1* with either *35S:AVP1* or *35S:PtVP1.1m* restored growth phenotype to the WT (Figures 3 and S2a–d available as Supplementary Data at *Tree Physiology* Online). All these results demonstrate that PtVP1.1(m) protein is a functional homolog of its *Arabidopsis* counterpart (AVP1).

Generation and molecular confirmation of transgenic poplar plants overexpressing PtVP1.1

In order to understand the function of *PtVP1.1* in salt tolerance, we introduced the construct containing *PtVP1.1m*, driven by the CaMV 35S promoter (Yang et al. 2008), into the genome of the aspen hybrid clone Shanxin yang by *Agrobacterium*-mediated transformation (Figure 4a). At least 20 independently regenerated kanamycin-resistant lines were obtained. Polymerase chain reaction analysis confirmed the integration of *PtVP1.1* into the genome of all the 11 randomly selected transgenic lines (Figure 4b). The relative expression levels of *PtVP1.1* in these transgenic lines were further quantified by quantitative real-time PCR (Figure 4c). Three independent transgenic lines (LP1, LP8 and LP9) with the same expression level as in the WT (LP8) or overexpression (LP1 and LP9) of *PtVP1.1* were selected for subsequent experiments. Measurement of isolated leaf microsomal fractions from WT and *PtVP1.1* transgenic plants revealed that transgenic plants overexpressing *PtVP1.1* (LP1 and LP9) had higher H^+-PPase activity than did the WT and LP8 plants (Figure 4d).

Overexpression of PtVP1.1 confers salt tolerance on transgenic poplar

To test whether overexpression of *PtVP1.1* would increase salt tolerance, we examined the effects of salt on the growth of transgenic poplars at whole-plant scale. At least 30 plants of WT and of each transgenic line (LP8, LP1 and LP9) were grown in a greenhouse. Overexpression of *PtVP1.1* did not change the overall development or plant morphology of transgenic poplar as transgenic lines LP8, LP1 and LP9 all grew well under normal growth conditions. There were no significant differences in growth phenotype (Figure 5a), plant height (Figure 5c), shoot fresh biomass (Figure 5d) or root fresh biomass (Figure 5e) between WT and transgenic plants. However, after 3 weeks of treatment with 150 mM NaCl, transgenic plants were considerably taller (Figure 5b and c) and produced significantly more shoot and root biomass than did the WT plants (Figure 5d and e). *PtVP1.1* overexpressing plants exhibited near-to-normal leaf color and less growth inhibition (Figure 5b–e). Compared with WT, the two overexpressing lines LP1 and LP9 produced 18 and 27% more fresh shoot mass, respectively, in the presence of

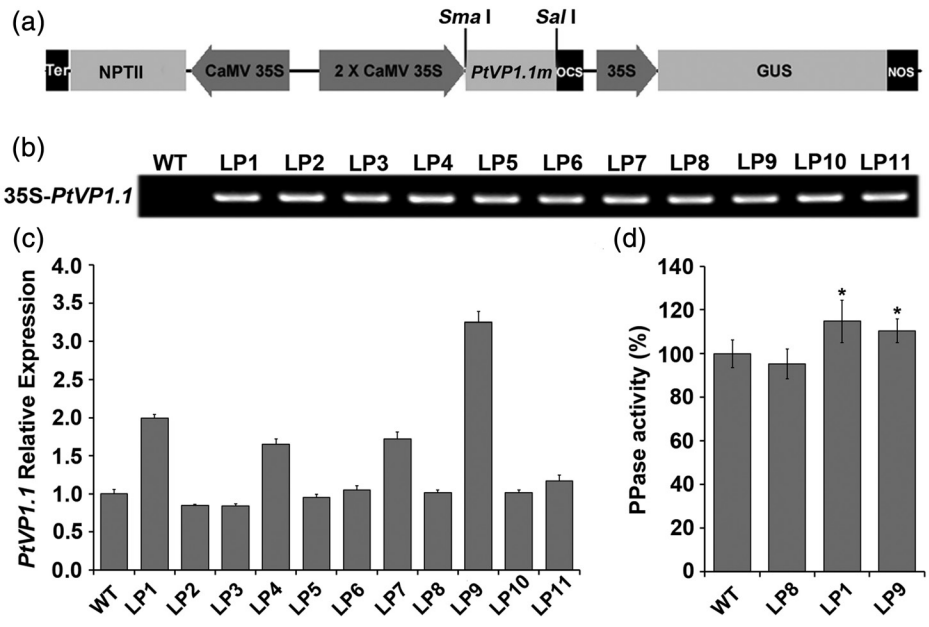

Figure 4. Plant expression vector and confirmation of transgenic poplar plants. (a) Schematic map of T-DNA region in the pCAMBIA2301-*PtVP1.1m* vector used for poplar transformation. Expression of *PtVP1.1m* is driven by the cauliflower mosaic virus 35S promoter. 35S: CaMV35S promoter; OCS, octopine synthase gene terminator; *NPTII*, neomycin phosphotransferase II gene; GUS, β-glucuronidase gene; NOS, NOS terminator. (b) PCR confirmation of independently regenerated kanamycin-resistant lines. (c) Quantitative real-time PCR analyses of *PtVP1.1* expression levels in different transgenic lines. WT, wild type; LP1–LP11, different transgenic lines. (d) H^+-PPase hydrolytic activity of three representative transgenic lines.

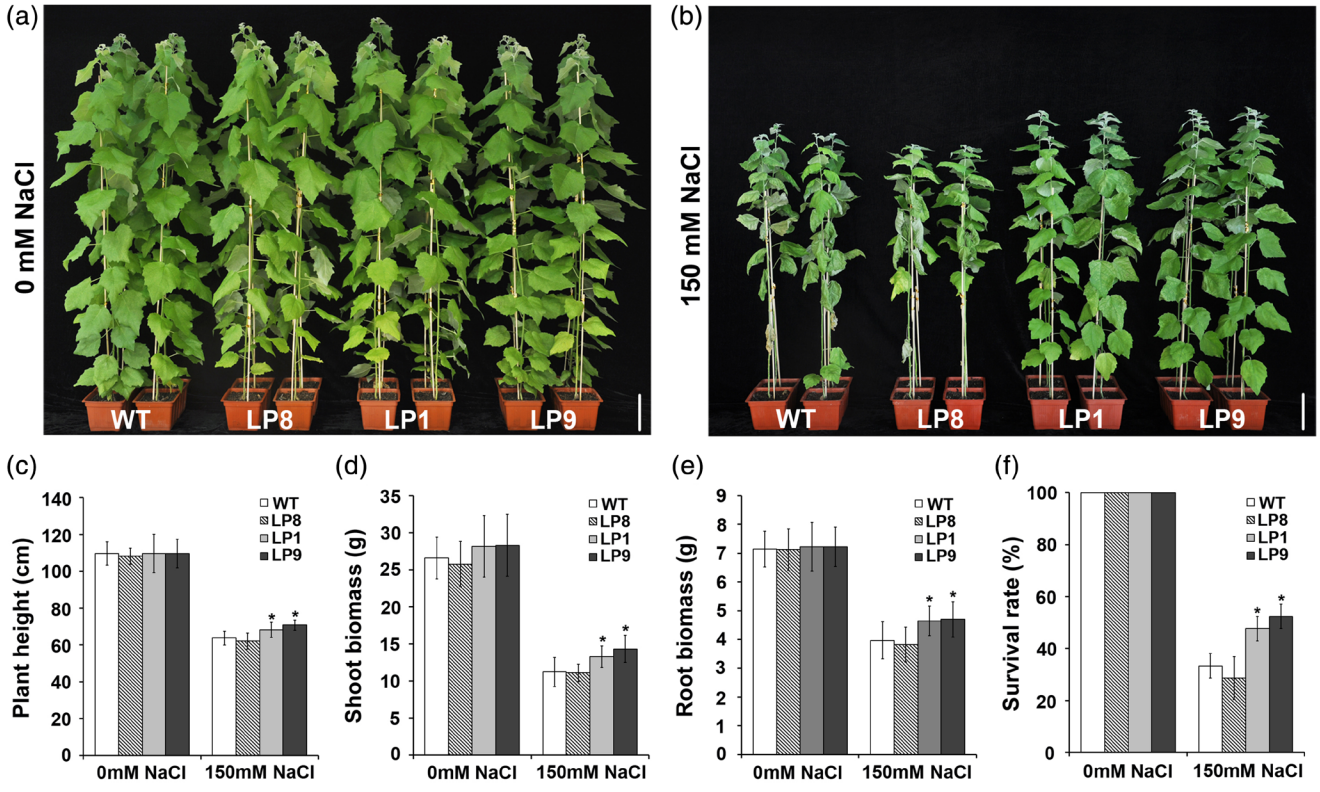

Figure 5. Overexpression of *PtVP1.1* enhances salt tolerance in transgenic poplar plants. (a and b) Effects of salinity on the growth of wild type (WT) and three independent transgenic lines LP8, LP1 and LP9. Six-week-old plants were treated with 0 or 150 mM NaCl for 21 days and then representative plants were chosen and photographed. Scale bars = 10 cm. (c) Plant height. (d) Shoot biomass. (e) Root biomass. (f) Survival rate. Values are means ± SD using 10 plants per line of two independent experiments. Asterisks indicate significant differences in comparison with the WT at $P < 0.05$ by Student's *t*-test.

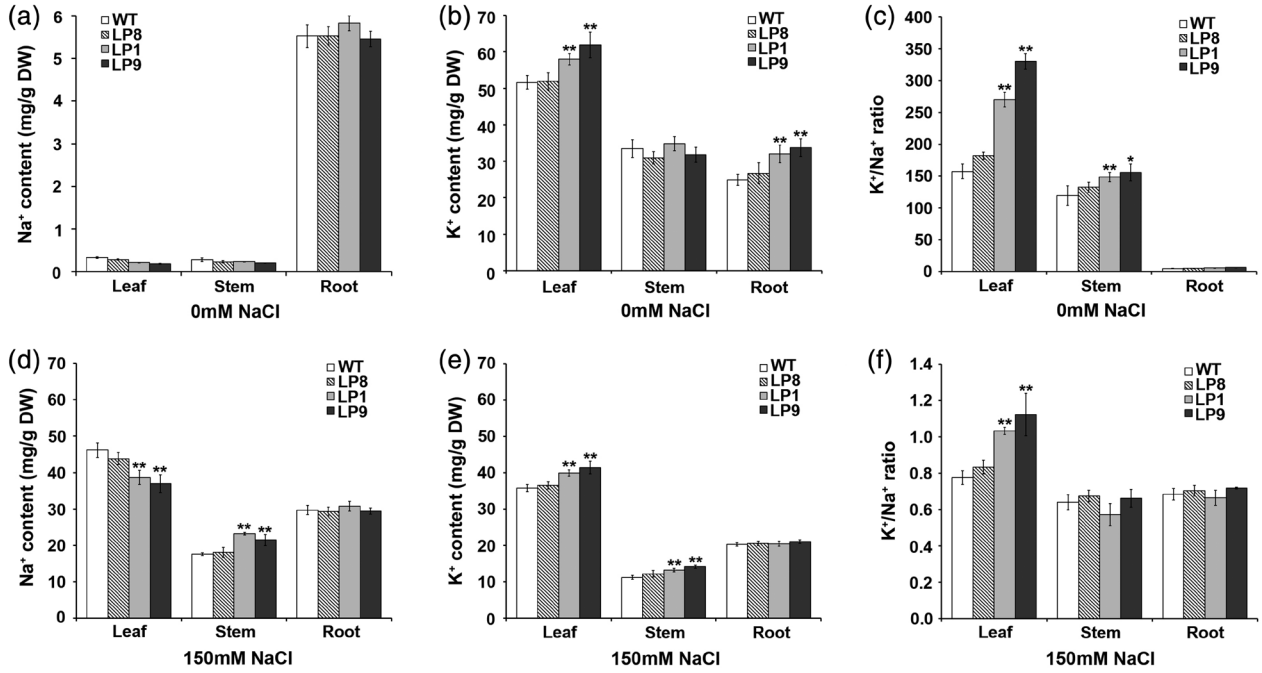

Figure 6. Ion content analyses. Wild-type (WT) and transgenic poplar plants (lines LP8, LP1 and LP9) were treated with 0 or 150 mM NaCl for 3 weeks. Plant materials were harvested and pooled as roots, stems and leaves for the measurement of Na^+ and K^+ contents. (a and d) Na^+ contents. (b and e) K^+ contents. (c and f) K^+/Na^+ ratios. Values are means ± SD of six plants per lines from two independent experiments. Asterisks indicate statistically significant difference in comparison with the WT (Student's *t*-test, *$0.01 < P < 0.05$, **$P < 0.01$).

150 mM NaCl (Figure 5d). Transgenic plants also showed a superior survival rate after the salt treatment (Figure 5f), and maintained relatively higher chlorophyll and lower MDA content in the leaves during the salt stress (see Figure S3a and b available as Supplementary Data at *Tree Physiology* Online). All these results indicate that overexpression of *PtVP1.1* enhanced salt tolerance in transgenic plants.

PtVP1.1 overexpression regulates tissue Na^+ and K^+ distribution in transgenic plants

In order to approach how *PtVP1.1* confers salt tolerance on transgenic poplar plants, we analyzed the concentrations of Na^+ and K^+ in different tissues of WT and transgenic plants grown under normal and salinity conditions. Consistent with our previous observation (Tang et al. 2014), under normal growth condition, poplar plants deposited most of Na^+ in the roots and accumulated more K^+ in the leaves (Figure 6a and b). And transgenic plants accumulated higher K^+ in roots and leaves but not in stems than did WT plants (Figure 6b). Under salt stress conditions, Na^+ content dramatically increased in all plant tissues of both WT and transgenic plants (Figure 6d), accompanied by a decrease in K^+ content (Figure 6e). However, Na^+ content in the leaves of *PtVP1.1* overexpressing lines (LP1 and LP9) was significantly lower (Figure 6d) whereas K^+ content (Figure 6e) and K^+/Na^+ ratio (Figure 6f) were dramatically higher than that in the leaves of WT and LP8 plants.

Na^+ efflux and H^+ influx are higher in the roots of transgenic poplar plants overexpressing PtVP1.1

The uptake, transport and compartmentalization of Na^+ are crucial for plants to survive under saline conditions. Using NMT, we examined the in vivo Na^+ and H^+ flux in the roots of WT and transgenic plants overexpressing PtVP1.1. Under normal (no-saline) conditions, the rates of Na^+ efflux and H^+ influx in the roots of transgenic plants were about the same as (or lower than) that in WT control plants. However, upon treatment with 100 mM NaCl, Na^+ efflux and H^+ influx in both *PtVP1.1* overexpressing lines LP1 and LP9 were significantly higher than

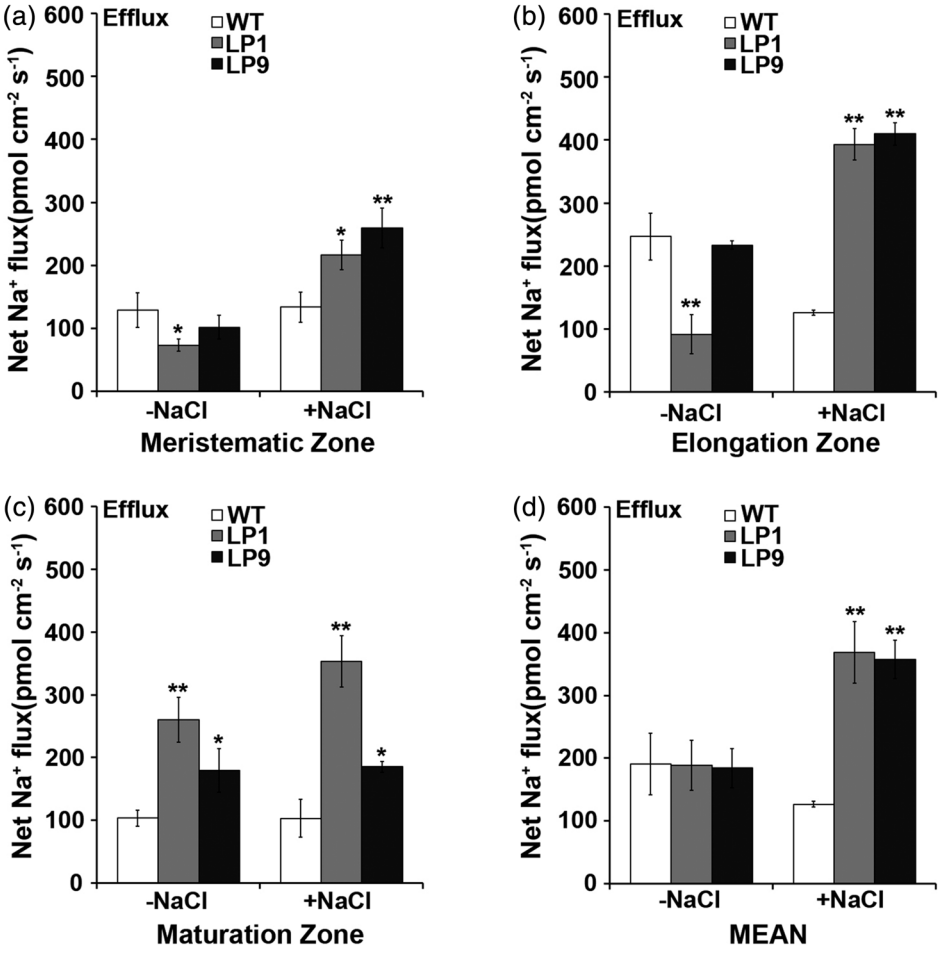

Figure 7. Net Na^+ flux test. Effect of salinity (100 mM NaCl) on net Na^+ efflux in the roots of transgenic lines (LP1, LP9) and WT plants. (a) Meristematic zone. (b) Elongation zone. (c) Maturation zone. (d) Mean net Na^+ efflux. Values are means ± SD from three independent experiments. Asterisks indicate statistically significant difference in comparison with the WT (Student's *t*-test, $*0.01 < P < 0.05$, $**P < 0.01$).

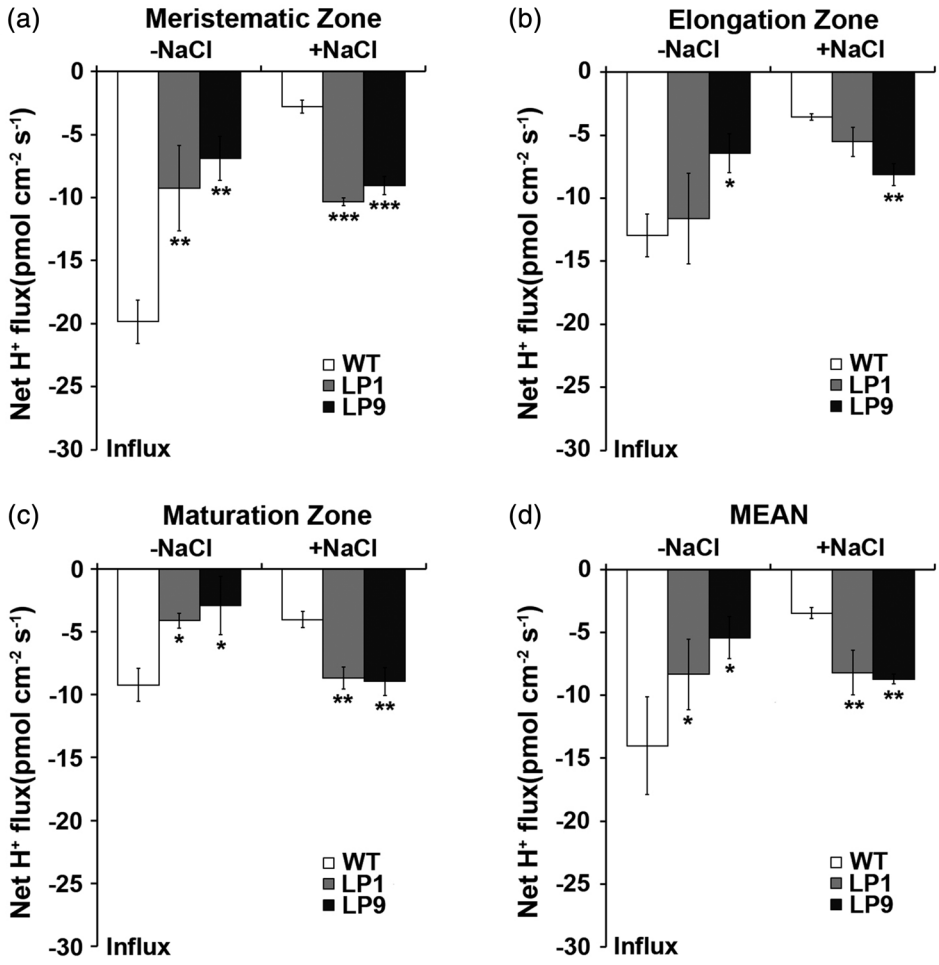

Figure 8. Net H^+ flux test. Effect of salinity (100 mM NaCl) on net H^+ influx in the roots of transgenic lines (LP1, LP9) and WT plants. (a) Meristematic zone. (b) Elongation zone. (c) Maturation zone. (d) Mean net H^+ influx. Values are means ± SD from three independent experiments. Asterisks indicate statistically significant difference in comparison with the WT (Student's *t*-test, $*0.01 < P < 0.05$, $**P < 0.01$).

WT in the measured regions of roots (meristematic, elongation and mature zones) (Figures 7 and 8). The increased Na^+ efflux and H^+ influx in transgenic plants could be the result of improved Na^+/H^+ exchange activity, as amiloride, a specific inhibitor of Na^+/H^+ antiporter, and Na_3VO_4, a specific inhibitor of H^+ pump, respectively, significantly reduced the salt-elicited Na^+ efflux (see Figure S4a–c available as Supplementary Data at *Tree Physiology* Online) and H^+ influx (see Figure S4d–f available as Supplementary Data at *Tree Physiology* Online) in the salt-stressed roots.

Discussion

As a perennial tree species, poplar may face different external abiotic stresses such as salt, drought and low temperature during its long lifetime course. Most poplar species are salt sensitive, except *Populus euphratica*, which has been selected due to its salt resistance (Chen and Polle 2010, Chen et al. 2014, Polle and Chen 2014), and crossed with other relevant cultivars to breed trees with increased salt tolerance. However, little success has been achieved due to the crossing barriers between different woody species. Therefore, genetic engineering has been employed as an alternative strategy to breed trees with improved salt tolerance (Hu et al. 2005, Wang et al. 2005, Takabe et al. 2008).

Higher plants have a large number of transport proteins that mediate Na^+ absorption, extrusion, translocation and sequestration (Horie and Schroeder 2004, Apse and Blumwald 2007) and a genetic regulatory network of signal transduction pathways to tightly regulate their response and adaption to environmental salt stress (Brinker et al. 2010, Janz et al. 2010). Despite the complexity of salt tolerance, introducing one single key gene, especially some regulatory genes involved in multiple signaling pathways, has successfully enhanced salt tolerance in transgenic plants (Zhang and Blumwald 2001, Yamaguchi and Blumwald 2005, Munns and Tester 2008, Pardo 2010). Among these genes, overexpression of *AVP1* and other plant type I H^+-PPase genes increased both salt and drought tolerance in different plant species (Gaxiola et al. 2001, Park et al. 2005, Gao et al. 2006, Zhao et al. 2006, Duan et al. 2007, Li et al. 2008,

2010, Lv et al. 2008, 2009, Bao et al. 2009). All these observations in herbaceous plants led us to postulate that overexpression of an H^+-PPase gene from woody plant might also confer stress tolerance on trees. To examine this hypothesis, we isolated a type I H^+-PPase homolog gene (*PtVP1.1*) from *P. trichocarpa* and investigated its possible function in *Arabidopsis* and transgenic poplar plants.

PtVP1.1 shares very high amino acid sequence identity with AVP1, and is similar to the other identified homologs such as OsVP1 and GhVP1 (Figure 1) (Zhao et al. 2006, Lv et al. 2008, 2009) that contain all the highly conserved domains (Drozdowicz and Rea 2001), indicating its possible role as a putative vacuolar H^+-PPase in *Populus*. Since *P. trichocarpa* has been used as an important model for trees (Jansson and Douglas 2007), a comparative study on the genetic effects of abiotic stress tolerance between Shanxin yang (*P. davidiana* × *P. bolleana*) and *A. thaliana* could shed light on the difference in the mechanisms of plant tolerance to environmental stress between herbaceous and woody plants. Previously, it was shown that in the four ecotypes of *A. thaliana*, salt tolerance of plants was positively related with *AVP1* expression. The two ecotypes of Ler and Ws, which showed a higher expression level of *AtAVP1* in both roots and shoots, also demonstrated higher tolerance to salinity when compared with ecotypes Col and C24, which had a lower level of both *AtAVP1* expression and salinity tolerance (Jha et al. 2010). In Shanxin yang, *PtVP1.1* mRNA was the most abundantly accumulated in xylem tissues and mature leaves (Figure 2). Therefore, the high expression of *PtVP1.1* in xylem tissues and mature leaves of wild-type Shanxin yang may imply a crucial role of *PtVP1.1* in salt tolerance of poplar plants.

Considering the high sequence homology of AVP1 and PtVP1.1, the physiological role of *PtVP1.1* was approached by *avp1* mutant analysis (see Figure S1a–d available as Supplementary Data at *Tree Physiology* Online). The most dramatic phenotypic changes in *avp1* mutant were the stunted growth, especially the root growth (Figures 3a, c, d and S2b–d available as Supplementary Data at *Tree Physiology* Online). Based on the previous report that an intragenic E229D gain-of-function allele of AVP1 had an in vitro-coordinated increase of both PPi hydrolytic activity and PPi-dependent H^+-translocation (Zhen et al. 1997), we generated a constitutively active form of PtVP1.1m by mutating the 227th amino acid Glu to Asp (Figure 4a). PtVP1.1m restored growth phenotype of *avp1* to the WT as did AVP1 (Figures 3 and S2a–d available as Supplementary Data at *Tree Physiology* Online), indicating that PtVP1.1m can be employed as a functional allele of PtVP1.1 in plants.

In terms of engineering of woody plants with improved salt tolerance, it is very important and practical to start with a relatively salt-tolerant variety. Different from the recently reported transgenic aspen T89, which shows hypersensitivity to as low a concentration of 17 mM NaCl (Zhou et al. 2014), Shanxin yang is a relatively more salt-tolerant hybrid aspen clone. Therefore, we constitutively overexpressed *PtVP1.1* in Shanxin yang, in which the native PtVP1.1 homolog (PdbVP1.1) shares very high amino acid (99.20%) identity with PtVP1.1 (Figures 4a–c and S5a available as Supplementary Data at *Tree Physiology* Online). As was been expected, the salt tolerance is significantly improved (Figure 5). Transgenic plants overexpressing *PtVP1.1* survived a concentration of 150 mM NaCl. To our knowledge, this is the highest concentration that has been reported so far in the tolerance of transgenic tree species. Previously, we overexpressed either PtSOS3 or PtCBL10, and transgenic poplar plants showed a tolerance to 100 mM NaCl in the same cultivar (Tang et al. 2014). The highest concentration of NaCl tested with transgenic T89 was 85 mM (Zhou et al. 2014).

It has been long suggested that both vascular long-distance Na^+ transport to different plant tissues and optimal Na^+ redistribution within the plant are critical in plant salt tolerance (Munns and Tester 2008). In addition to maintaining vacuolar pH and building up H^+ gradient, AVP1 also functions in auxin transport and consequently auxin-dependent development (Li et al. 2005). In transgenic plants overexpressing *PtVP1.1*, the salt-tolerant phenotype was associated with a lower Na^+ content and a higher K^+ content in leaf tissues relative to WT plants (Figure 6). Data presented here are consistent with the earlier report that transgenic plants overexpressing SOS1 accumulated less Na^+ in the shoot upon treatment with salt (Shi et al. 2003). A higher K^+–Na^+ ratio associated with salt tolerance has been reported by many researchers (Luo et al. 2009, 2011, Yang et al. 2015).

In creeping bentgrass (*A. stolonifera* L.), heterologous expression of *AVP1* conferred increased salt tolerance and Na^+ accumulation (Li et al. 2010). In tomato, co-expression of *AVP1* and *Pennisetum glaucum* vacuolar Na^+/H^+ antiporter *PgNHX1* also conferred enhanced salt tolerance to the transformed tomato compared with the WT. Transgenic tomato plants grew well in the presence of 200 mM NaCl, retained more chlorophyll, produced more proline and accumulated higher Na^+ in their leaf tissue as a response to salt stress (Bhaskaran and Savithramma 2011). Conversely, we observed that transgenic plants overexpressing *PtVP1.1* accumulated lower Na^+ content in their leaf tissue in the presence of 150 mM NaCl (Figure 6d). Similar results were also observed in our previous study with transgenic poplar overexpressing *PtCBL10A* or *PtCBL10B* (Tang et al. 2014). In poplar, unlike *PtSOS3* which is mainly expressed in root tissues, *PtCBL10* genes were preferentially expressed in shoots (Tang et al. 2010, 2014). Therefore, we hypothesize that, to maintain an optimal K^+/Na^+ ratio and thereby confer increased salt tolerance to transgenic plants, PtSOS2 may interact with PtCBL10s and/or PtSOS3 in different tissues/organs to activate the plasma membrane-located Na^+/H^+ antiporter PtSOS1 and/or tonoplast-located Na^+/H^+ antiporter(s) such as PtNHX1 (Tang et al. 2010, 2014). Indeed, various subcellular

localizations such as vacuolar and plasma membrane of AVP1 in different cell types have been reported (Long et al. 1995, Baltscheffsky et al. 1999, Ratajczak et al. 1999, Drozdowicz and Rea 2001, Li et al. 2005, Segami et al. 2014). In this study, Na^+ content was lower in the leaves but higher in the stems of transgenic plants overexpressing *PtVP1.1* when compared with the WT controls upon treatment with salt stress (Figure 6d). Furthermore, transient expression of CFP-PtVP1.1 in poplar mesophyll protoplasts and *Arabidopsis* PSBD protoplasts indicated that the fusion protein was mainly localized to the plasma membrane, with a minor localization to the cytosol (see Figure S5b and c available as Supplementary Data at *Tree Physiology* Online). Therefore, the decreased Na^+ content in transgenic plant overexpressing *PtVP1.1* can be possibly ascribed to the increased PtSOS1 Na^+/H^+ exchange activity driven by the enhanced H^+ gradient in the leaf tissues. This hypothesis is also supported by the unchanged *PtSOS1* transcription in both transgenic lines overexpressing *PtVP1.1* (see Figure S6a available as Supplementary Data at *Tree Physiology* Online) and the SOS1-dependent salt tolerance triggered by H^+-PPase up-regulation in *Arabidopsis*. Enhanced AVP1 protein level is post-translationally regulated by SOS1 (Undurraga et al. 2012). Future work such as systematic examination of the native subcellular location(s) of PtVP1.1 in different tissue cells will be required to fully understand the precise action of PtVP1.1 in poplar.

Another interesting observation is that transgenic plants overexpressing *PtVP1.1* showed a higher K^+ content and K^+/Na^+ ratio in leaf tissues than did the WT under both no-salt and salty conditions (Figure 6b, c, e and f). Translocation of K^+ into the lumen can be regulated by vacuolar NHX-type K^+/H^+ antiporters such as NHX1 (Leidi et al. 2010, Bassil et al. 2011, Barragán et al. 2012). Therefore, a possible explanation is that more K^+ accumulated in the vacuole as a compensation for the loss of other mineral ions. Therefore, it would be interesting to determine how K^+/H^+ exchange at the tonoplast was altered in the transgenic plants overexpressing *PtVP1.1*.

Now that salt tolerance was mainly exhibited in the aerial parts of transgenic plants overexpressing *PtVP1.1* (Figure 5b), and consistent with the reduced Na^+ content in leaf tissues (Figure 6d), results in this work indicate that overexpression of *PtVP1.1* might have promoted the active efflux of Na^+ in roots and thereby altered its distribution to leaves. In transgenic plants, the lower Na^+ content in mature leaves was associated with an increased Na^+ efflux in the roots (Figure 7). To further assess whether the improved Na^+/H^+ exchange activity was a consequence of increased H^+ gradient in these transgenic plants, influx of H^+ in roots was also investigated. Four-week-old seedlings grown on MS medium, which were much more sensitive to salt than the soil-grown plants, were used and exposed to salt solution directly for a long time. To make sure the roots would not die before the end of salt treatment, we lowered the NaCl concentration from 150 to 100 mM. Similar to the rise of Na^+ efflux, influx of H^+ was also dramatically elevated as a response to salt stress (Figure 8). To ensure that the relatively higher Na^+ efflux and H^+ influx were not due to passive diffusion, amiloride, an inhibitor of Na^+/H^+ antiporter, and Na_3VO_4, a specific inhibitor of H^+ pump, was used in our study. Pretreatment with amiloride and Na_3VO_4 efficaciously restrained root Na^+ efflux and H^+ influx in transgenic plants, respectively (see Figure S4a–f available as Supplementary Data at *Tree Physiology* Online), suggesting that the increased Na^+ efflux and H^+ influx were indeed a result of improved Na^+/H^+ exchange and H^+ translocation activity across the vacuolar and/or plasma membrane. We also examined the expression levels of Na^+/H^+ antiporter genes (see Figure S6a–d available as Supplementary Data at *Tree Physiology* Online), and found that the transcripts of both *PtNHX2* and *PtNHX4* were up-regulated in transgenic plants overexpressing *PtVP1.1* upon treatment with 150 mM NaCl, implying that the increased Na^+/H^+ exchange activities could be a result of both improved expression and activity of these Na^+/H^+ transporters (see Figure S6a–d available as Supplementary Data at *Tree Physiology* Online).

Salt stress can adversely affect photosynthesis and the electron transport system (Demmig-Adams and Adams 1992, Allakhverdiev et al. 2002). Under high saline conditions, excessive cytoplasmic Na^+ gives rise to an imbalanced cellular ion contents, leading to the production of reactive oxygen species (ROS) such as singlet oxygen, H_2O_2 and $O_2^{\cdot-}$, which causes chlorophyll degradation and membrane lipid peroxidation (Hasegawa et al. 2000, Yasar et al. 2006). To evaluate the ability of transgenic plants to alleviate salt effects on photosynthesis, chlorophyll and MDA contents were examined in WT and transgenic plants overexpressing *PtVP1.1*. The loss of chlorophyll and the accumulation of MDA in the leaves of transgenic plants were significantly lower than those in the control set during exposure to salinity (see Figure S3a and b available as Supplementary Data at *Tree Physiology* Online). Metabolism of ROS is controlled by a complex set of antioxidant enzymes. Catalase (CAT) along with superoxide dismutase (SOD) and ascorbate peroxidases (APX) are the major enzymes responsible for ROS scavenging (Mittler 2002). Although the expression of SOD and APX was largely unaffected in WT and transgenic plants after being treated with 150 mM NaCl (data not shown), transcription of CAT, which has been considered to be especially important for detoxification of H_2O_2 formed during photosynthesis and photorespiration (Willekens et al. 1997), was dramatically up-regulated in transgenic plants overexpressing *PtVP1.1* (see Figure S6e available as Supplementary Data at *Tree Physiology* Online). Transcription of a proline biosynthesis gene *PtP5CS1* was also up-regulated (see Figure S6f available as Supplementary Data at *Tree Physiology* Online). All these results suggest that the photosynthetic machinery is protected from deleterious salt effects, possibly by the reduced Na^+ accumulation in transgenic plants.

In conclusion, data presented in this study demonstrate that constitutive overexpression of *PtVP1.1* in poplar increased salt tolerance. Overexpression of *PtVP1.1* enhanced the H^+-PPase activity and Na^+ efflux, thereby reducing Na^+ accumulation in transgenic plants, leading to improved tolerance to salt in these plants. The substantially increased resistance to salt stress reported here provides a promising strategy for engineering salt-tolerant trees by constitutively expressing the *PtVP1.1* gene.

Supplementary data

Supplementary data for this article are available at *Tree Physiology* Online.

Acknowledgments

We thank Prof. Gui-Feng Liu (Northeast Forestry University, China) for kindly providing us the Shanxin yang (*P. davidiana* × *P. bolleana*) clone and Mr Jiehui Guanzhang (University of Toronto, Canada) for the critical reading and comments on this manuscript.

Conflict of interest

None declared.

Funding

This work has been jointly supported by the following grants: the National Natural Science Foundation of China (31171169, 31100212, 31371228, 31370670, 31270654, 31470661); the National Mega Project of GMO Crops (2013ZX08001003-007, 2013ZX08004002-006, 2014ZX0800942B); the Strategic Priority Research Program of the Chinese Academy of Sciences (XDA08030108); the Natural Science Foundation of Shandong Province of China (ZR2014CM004); the Research Project of the Chinese Ministry of Education (113013A); the Program for Changjiang Scholars and Innovative Research Teams in University (IRT13047); the key project for Oversea Scholars by the Ministry of Human Resources and Social Security of China (2012001); the Program of Introducing Talents of Discipline to Universities (111 Project B13007); the Natural Science Foundation of Jiangsu Province of China (BK2012306); and Shanghai Key Laboratory of Bio-Energy Crops.

References

Allakhverdiev SI, Nishiyama Y, Miyairi S, Yamamoto H, Inagaki N, Kanesaki Y, Murata N (2002) Salt stress inhibits the repair of photodamaged photosystem II by suppressing the transcription and translation of *psbA* genes in *Synechocystis*. Plant Physiol 130:1443–1453.

Apse MP, Blumwald E (2007) Na^+ transport in plants. FEBS Lett 581:2247–2254.

Baltscheffsky M, Schultz A, Baltscheffsky H (1999) H^+-proton-pumping inorganic pyrophosphatase: a tightly membrane-bound family. FEBS Lett 452:121–127.

Bao AK, Wang SM, Wu GQ, Xi JJ, Zhang JL, Wang CM (2009) Overexpression of the *Arabidopsis* H^+-PPase enhanced resistance to salt and drought stress in transgenic alfalfa (*Medicago sativa* L.). Plant Sci 176:232–240.

Barragán V, Leidi EO, Andrés Z, Rubio L, De Luca A, Fernandez JA, Cubero B, Pardo JM (2012) Ion exchangers NHX1 and NHX2 mediate active potassium uptake into vacuoles to regulate cell turgor and stomatal function in *Arabidopsis*. Plant Cell 24:1127–1142.

Bassil E, Tajima H, Liang YC et al. (2011) The *Arabidopsis* Na^+/H^+ antiporters NHX1 and NHX2 control vacuolar pH and K^+ homeostasis to regulate growth, flower development, and reproduction. Plant Cell 23:3482–3497.

Bhaskaran S, Savithramma DL (2011) Co-expression of *Pennisetum glaucum* vacuolar Na^+/H^+ antiporter and *Arabidopsis* H^+-pyrophosphatase enhances salt tolerance in transgenic tomato. J Exp Bot 62:5561–5570.

Blumwald E, Gelli A (1997) Secondary inorganic ion transport at the tonoplast. In: Sanders LA (ed.) The plant vacuole: advances in botanical research. Academic Press, San Diego, CA, pp 401–417.

Brinker M, Brosché M, Vinocur B et al. (2010) Linking the salt transcriptome with physiological responses of a salt-resistant *Populus* species as a strategy to identify genes important for stress acclimation. Plant Physiol 154:1697–1709.

Chen S, Polle A (2010) Salinity tolerance of *Populus*. Plant Biol 12:317–333.

Chen S, Hawighorst P, Sun J, Polle A (2014) Salt tolerance in *Populus*: significance of stress signaling networks, mycorrhization, and soil amendments for cellular and whole-plant nutrition. Environ Exp Bot 107:113–124.

Chen Z, Newman I, Zhou M, Mendham N, Zhang G, Shabala S (2005) Screening plants for salt tolerance by measuring K^+ flux: a case study for barley. Plant Cell Environ 28:1230–1246.

Clough SJ, Bent AF (1998) Floral dip: a simplified method for *Agrobacterium*-mediated transformation of *Arabidopsis thaliana*. Plant J 16:735–743.

Cuin TA, Bose J, Stefano G, Jha D, Tester M, Mancuso S, Shabala S (2011) Assessing the role of root plasma membrane and tonoplast Na^+/H^+ exchangers in salinity tolerance in wheat: in planta quantification methods. Plant Cell Environ 34:947–961.

Demmig-Adams B, Adams WW (1992) Photoprotection and other responses of plants to high light stress. Annu Rev Plant Physiol Plant Mol Biol 43:599–626.

Drozdowicz YM, Rea PA (2001) Vacuolar H(+) pyrophosphatases: from the evolutionary backwaters into the mainstream. Trends Plant Sci 6:206–211.

Duan XG, Yang AF, Gao F, Zhang SL, Zhang JR (2007) Heterologous expression of vacuolar H^+-PPase enhances the electrochemical gradient across the vacuolar membrane and improves tobacco cell salt tolerance. Protoplasma 232:87–95.

Gao F, Gao Q, Duan XG, Yue GD, Yang AF, Zhang JR (2006) Cloning of an H^+-PPase gene from *Thellungiella halophila* and its heterologous expression to improve tobacco salt tolerance. J Exp Bot 57:3259–3270.

Gaxiola RA, Li J, Undurraga S, Dang LM, Allen GJ, Alper SL, Fink GR (2001) Drought- and salt-tolerant plants result from overexpression of the AVP1 H^+-pump. Proc Natl Acad Sci USA 98:11444–11449.

Hasegawa PM, Bressan RA, Zhu JK, Bohnert HJ (2000) Plant cellular and molecular responses to high salinity. Annu Rev Plant Physiol Plant Mol Biol 51:463–499.

Horie T, Schroeder JI (2004) Sodium transporters in plants. Diverse genes and physiological functions. Plant Physiol 136:2457–2462.

Hu L, Lu H, Liu Q, Chen X, Jiang X (2005) Overexpression of *mtlD* gene in transgenic *Populus tomentosa* improves salt tolerance through accumulation of mannitol. Tree Physiol 25:1273–1281.

Jansson S, Douglas CJ (2007) *Populus*: a model system for plant biology. Annu Rev Plant Biol 58:435–458.

Janz D, Behnke K, Schnitzler JP, Kanawati B, Schmitt-Kopplin P, Polle A (2010) Pathway analysis of the transcriptome and metabolome of salt sensitive and tolerant poplar species reveals evolutionary adaption of stress tolerance mechanisms. BMC Plant Biol 10:150–166.

Jha D, Shirley N, Tester M, Roy SJ (2010) Variation in salinity tolerance and shoot sodium accumulation in *Arabidopsis* ecotypes linked to differences in the natural expression levels of transporters involved in sodium transport. Plant Cell Environ 33:793–804.

Kasai M, Nakamura T, Kudo N, Sato H, Maeshima M, Sawada S (1998) The activity of the root vacuolar H^+-pyrophosphatase in rye plants grown under conditions deficient in mineral nutrients. Plant Cell Physiol 39:890–894.

Leidi EO, Barragán V, Rubio L et al. (2010) The AtNHX1 exchanger mediates potassium compartmentation in vacuoles of transgenic tomato. Plant J 61:495–506.

Li B, Wei A, Song C, Li N, Zhang JR (2008) Heterologous expression of the *TsVP* gene improves the drought resistance of maize. Plant Biotechnol J 6:146–159.

Li J, Yang H, Peer WA et al. (2005) *Arabidopsis* H^+-PPase AVP1 regulates auxin-mediated organ development. Science 310:121–125.

Li J, Bao S, Zhang Y et al. (2012) *Paxillus involutus* strains MAJ and NAU mediate K^+/Na^+ homeostasis in ectomycorrhizal *Populus* × *canescens* under sodium chloride stress. Plant Physiol 159:1771–1786.

Li Z, Baldwin CM, Hu Q, Liu H, Luo H (2010) Heterologous expression of *Arabidopsis* H^+-pyrophosphatase enhances salt tolerance in transgenic creeping bentgrass (*Agrostis stolonifera* L.). Plant Cell Environ 33:272–289.

Lichtenthaler HK (1987) Chlorophylls and carotenoids: pigments of photosynthetic biomembranes. Methods Enzymol 148:350–382.

Long AR, Williams LE, Nelson SJ, Hall JL (1995) Localization of membrane pyrophosphatase activity in *Ricinus communis* seedlings. J Plant Physiol 146:629–638.

Luo ZB, Janz D, Jiang XN, Gobel C, Wildhagen H, Tan YP, Rennenberg H, Feussner I, Polle A (2009) Upgrading root physiology for stress tolerance by ectomycorrhizas: insights from metabolite and transcriptional profiling into reprogramming for stress anticipation. Plant Physiol 151:1902–1917.

Luo ZB, Li K, Gai Y, Göbel C, Wildhagen H, Jiang XN, Feußner I, Rennenberg H, Polle A (2011) The ectomycorrhizal fungus (*Paxillus involutus*) modulates leaf physiology of poplar towards improved salt tolerance. Environ Exp Bot 72:304–311.

Lv S, Zhang K, Gao Q, Lian L, Song Y, Zhang JR (2008) Overexpression of an H^+-PPase gene from *Thellungiella halophila* in cotton enhances salt tolerance and improves growth and photosynthetic performance. Plant Cell Physiol 49:1150–1164.

Lv SL, Lian LJ, Tao PL, Li ZX, Zhang KW, Zhang JR (2009) Overexpression of *Thellungiella halophila* H^+-PPase (*TsVP*) in cotton enhances drought stress resistance of plants. Planta 229:899–910.

Maeshima M (2000) Vacuolar H^+-pyrophosphatase. Biochim Biophys Acta 1465:37–51.

Miao Y, Jiang L (2007) Transient expression of fluorescent fusion proteins in protoplasts of suspension cultured cells. Nat Protoc 2:2348–2353.

Mishra S, Alavilli H, Lee BH, Panda SK, Sahoo L (2015) Cloning and characterization of a novel vacuolar Na^+/H^+ antiporter gene (*VuNHX1*) from drought hardy legume, cowpea for salt tolerance. Plant Cell Tissue Organ Cult 120:19–33.

Mittler R (2002) Oxidative stress, antioxidants and stress tolerance. Trends Plant Sci 7:405–410.

Munns R, Tester M (2008) Mechanisms of salinity tolerance. Annu Rev Plant Biol 59:651–681.

Murashige T, Skoog F (1962) A revised medium for rapid growth and bio assays with tobacco tissue cultures. Physiol Plant 15:473–497.

Paez-Valencia J, Sanchez-Lares J, Marsh E et al. (2013) Enhanced proton translocating pyrophosphatase activity improves nitrogen use efficiency in Romaine Lettuce. Plant Physiol 161:1557–1569.

Pardo JM (2010) Biotechnology of water and salinity stress tolerance. Curr Opin Plant Biol 21:185–196.

Park S, Li J, Pittman JK, Berkowitz GA, Yang H, Undurraga S, Morris J, Hirschi KD, Gaxiola RA (2005) Up-regulation of a H^+-pyrophosphatase (H^+-PPase) as a strategy to engineer drought-resistant crop plants. Proc Natl Acad Sci USA 102:18830–18835.

Polle A, Chen S (2014) On the salty side of life: molecular, physiological and anatomical adaptation and acclimation of trees to extreme habitats. Plant Cell Environ. doi:10.1111/pce.12440.

Ratajczak R, Hinz G, Robinson DG (1999) Localization of pyrophosphatase in membranes of cauliflower inflorescence cells. Planta 208:205–211.

Rea PA, Poole RJ (1985) Proton-translocating inorganic pyrophosphatase in red beet (*Beta vulgaris* L.) tonoplast vesicles. Plant Physiol 77:46–52.

Rea PA, Kim Y, Sarafian V, Poole RJ, Davies JM, Sanders D (1992) Vacuolar H+-translocating pyrophosphatases: a new category of ion translocase. Trends Biochem Sci 17:348–353.

Segami S, Makino S, Miyake A, Asaoka M, Maeshima M (2014) Dynamics of vacuoles and H^+-Pyrophosphatase visualized by monomeric green fluorescent protein in *Arabidopsis*: artifactual bulbs and native intravacuolar spherical structures. Plant Cell 26:3416–3434.

Shi H, Lee B, Wu SJ, Zhu JK (2003) Overexpression of a plasma membrane Na^+/H^+ antiporter gene improves salt tolerance in *Arabidopsis thaliana*. Nat Biotechnol 21:81–85.

Sun J, Chen S, Dai S et al. (2009*a*) NaCl-induced alternations of cellular and tissue ion fluxes in roots of salt-resistant and salt-sensitive poplar species. Plant Physiol 149:1141–1153.

Sun J, Dai S, Wang R et al. (2009*b*) Calcium mediates root K^+/Na^+ homeostasis in poplar species differing in salt tolerance. Tree Physiol 29:1175–1186.

Takabe T, Uchida A, Shinagawa F et al. (2008) Overexpression of *DnaK* from a halotolerant cyanobacterium *Aphanothece halophytica* enhances growth rate as well as abiotic stress tolerance of poplar plants. Plant Growth Regul 56:265–273.

Tang RJ, Liu H, Bao Y, Lv QD, Yang L, Zhang HX (2010) The woody plant poplar has a functionally conserved salt overly sensitive pathway in response to salinity stress. Plant Mol Biol 74:367–380.

Tang RJ, Liu H, Yang Y, Yang L, Gao XS, Garcia VJ, Luan S, Zhang HX (2012) Tonoplast calcium sensors CBL2 and CBL3 control plant growth and ion homeostasis through regulating V-ATPase activity in *Arabidopsis*. Cell Res 22:1650–1665.

Tang RJ, Yang Y, Yang L, Liu H, Wang CT, Yu MM, Gao XS, Zhang HX (2014) Poplar calcineurin B-like proteins PtCBL10A and PtCBL10B regulate shoot salt tolerance through interaction with PtSOS2 in the vacuolar membrane. Plant Cell Environ 37:573–588.

Undurraga SF, Santos MP, Paez-Valencia J, Yang H, Hepler PK, Facanha AR, Hirschi KD, Gaxiola RA (2012) *Arabidopsis* sodium dependent and independent phenotypes triggered by H^+-PPase up-regulation are SOS1 dependent. Plant Sci 183:96–105.

Wang BS, Zhao KF (1995) Comparison of extractive methods of Na^+, K^+ in wheat leaves. Plant Physiol Commun 31:50–52.

Wang B, Lüttge U, Ratajczak R (2001) Effects of salt treatment and osmotic stress on V-ATPase and V-PPase in leaves of the halophyte *Suaeda salsa*. J Exp Bot 52:2355–2365.

Wang HH, Wang CT, Liu H, Tang RJ, Zhang HX (2011) An efficient *Agrobacterium*-mediated transformation and regeneration system for leaf explants of two elite aspen hybrid clones *Populus alba* × *P. berolinensis* and *Populus davidiana* × *P. bolleana*. Plant Cell Rep 30:2037–2044.

Wang S, Chen Q, Wang W, Wang X, Lu M (2005) Salt tolerance conferred by over-expression of *OsNHX1* gene in Poplar 84K. Chin Sci Bull 50:224–228.

Willekens H, Chamnongpol S, Davey M, Schraudner M, Langebartels C, Van Montagu M, Inzé D, Van Camp W (1997) Catalase is a sink for H_2O_2 and is indispensable for stress defence in C_3 plants. EMBO J 16:4806–4816.

Yamaguchi T, Blumwald E (2005) Developing salt-tolerant crop plants: challenges and opportunities. Trends Plant Sci 10:615–620.

Yang H, Knapp J, Koirala P, Rajagopal D, Peer WA, Silbart LK, Murphy A, Gaxiola RA (2007) Enhanced phosphorus nutrition in monocots and dicots over-expressing a phosphorus-responsive type I H^+-pyrophosphatase. Plant Biotech J 5:735–745.

Yang L, Tang RJ, Zhu JQ, Liu H, Mueller-Roeber B, Xia HJ, Zhang HX (2008) Enhancement of stress tolerance in transgenic tobacco plants constitutively expressing Atlpk2β, an inositol polyphosphate 6-/3-kinase from *Arabidopsis thaliana*. Plant Mol Biol 66:329–343.

Yang Y, Tang RJ, Jiang CM et al. (2015) Overexpression of the *PtSOS2* gene improves tolerance to salt stress in transgenic poplar plants. Plant Biotechnol J. doi:10.1111/pbi.12335.

Yasar F, Kusvuran S, Ellialtıoğlu S (2006) Determination of anti-oxidant activities in some melon (*Cucumis melo* L.) varieties and cultivars under salt stress. J Hortic Sci Biotechnol 81:627–630.

Zhang HX, Blumwald E (2001) Transgenic salt-tolerant tomato plants accumulate salt in foliage but not in fruit. Nat Biotechnol 19:765–768.

Zhao FY, Zhang XJ, Li PH, Zhao YX, Zhang H (2006) Co-expression of the *Suaeda salsa SsNHX1* and *Arabidopsis AVP1* confer greater salt tolerance to transgenic rice than the single *SsNHX1*. Mol Breed 17: 341–353.

Zhao SJ, Xu CC, Zhou Q, Meng QW (1994) Improvements of method for measurement of malondialdehyde in plant tissues. Plant Physiol Commun 30:207–210 (in Chinese).

Zhen RG, Kim EJ, Rea PA (1997) Acidic residues necessary for pyrophosphate-energized pumping and inhibition of the vacuolar H^+-pyrophosphatase by *N,N′*-dicyclohexylcarbodiimide. J Biol Chem 272: 22340–22348.

Zhou J, Wang JJ, Bi YF, Wang LK, Tang LZ, Yu X, Ohtani M, Demura T, Zhuge Q (2014) Overexpression of *PtSOS2* enhances salt tolerance in transgenic poplars. Plant Mol Biol Rep 32:185–197.